First Measurement of Pure Electron Shakeoff in the β Decay of Trapped 6He+ Ions

C. Couratin, P. Velten, X. Fléchard, E. Liénard, G. Ban, A. Cassimi, P. Delahaye, D. Dominique Durand, D. Hennecart, F. Mauger, et al.

First measurement of pure electron shake-off in the β decay of trapped $^6He^+$ ions

C. Couratin,[1] Ph. Velten,[1] X. Fléchard,[1,*] E. Liénard,[1] G. Ban,[1] A. Cassimi,[2]
P. Delahaye,[3] D. Durand,[1] D. Hennecart,[2] F. Mauger,[1] A. Méry,[2] O. Naviliat-Cuncic,[1,4]
Z. Patyk,[5] D. Rodríguez,[6] K. Siegień-Iwaniuk,[5] and J-C. Thomas[3]

[1]*LPC Caen, ENSICAEN, Université de Caen Basse Normandie, CNRS/IN2P3-ENSI, Caen, France*
[2]*CIMAP, CEA/CNRS/ENSICAEN, BP 5133, F-14070, Caen, France*
[3]*GANIL, CEA/DSM-CNRS/IN2P3, Caen, France*
[4]*NSCL and Department of Physics and Astronomy, Michigan State University, East-Lansing, MI, USA*
[5]*National Centre for Nuclear Research, Hoza 69, PL-00-681 Warsaw, Poland*
[6]*Departemento de Física Atómica, Molecular y Nuclear, Universitad de Granada, Granada, Spain*

(Dated: May 14, 2012)

The electron shake-off probability of $^6Li^{2+}$ ions resulting from the β^- decay of $^6He^+$ ions has been measured with high precision using a specially designed recoil ion spectrometer. This is the first measurement of a pure electron shake-off following nuclear β decay, not affected by multi-electron processes such as Auger cascades. In this ideal textbook case for the application of the sudden approximation, the experimental ionisation probability was found to be $P_{so}^{exp} = 0.02339(36)$ in perfect agreement with simple quantum mechanical calculations.

PACS numbers: 23.40.-s, 31.15.ac, 34.50.Fa, 37.10.Ty

Electron shake-off (SO) and shake-up (SU) are fundamental atomic processes in which a bound electron is excited into the continuum or in a new orbital, resulting from a sudden change of the central potential. This monopole ionization or excitation may be due to a modification of the nuclear charge, like in nuclear β decay, nuclear electron capture, internal conversion and alpha decay [1], or to the creation of a vacancy in an atomic inner shell induced by collisions with charged particles [2] or by photo-ionization [3, 4]. The probabilities of these processes can be calculated in the framework of the sudden approximation (SA). The accuracy of the calculation depends on how fast the central potential changes as compared with the relaxation time of electrons in the new core potential. Nuclear β decay offers ideal conditions to test such calculations since the change in the central potential occurs in less than 10^{-18} s, which is the transit time of the emitted β particles through the orbital electron cloud.

The first calculations of SO and SU probabilities following β decay [5–7] used hydrogen like wave functions. More sophisticated calculations were performed using numerical self-consistent wave functions for many-electron atoms [8]. The comparison between calculations and experiments is usually difficult [9] since secondary processes, like the emission of Auger electrons, contribute to the final charge state of the daughter ions. The simplest case investigated so far for such comparisons was the SO following the β decay of ^{6}He atoms [10]. The single ionization probability of the daughter $^6Li^+$ ions was there found in good agreement with a former measurement [11] but the double ionization probability was overestimated by almost one order of magnitude. This stresses the difficulties of treating such systems, even with only two active electrons.

For radioactive species with one active electron, such as $^6He^+$ ions, electron-electron correlations and secondary relaxation processes are absent, leaving only two possible mechanisms for the daughter ionization. The dominant one, the electron SO, is caused by both the rapid change of the nuclear charge and the sudden recoil velocity acquired by the daughter nucleus resulting from β decay. In ^{6}He decay, the recoil energy can reach 1.4 keV so that the recoil effect can have a sizable impact on the SO probabilities [8]. The second ionization mechanism is a direct collision, in which the β particle knocks out the bound electron. Its probability depends on the energy of the β particle, ($E_{max} = 3.5$ MeV), as compared to the 54.4 eV electron binding energy [5]. The direct collision is thus expected to have a very small contribution in the $^6Li^{2+}$ ionization following the $^6He^+$ β decay.

$^6Li^{2+}$ ions produced after β decay offer therefore an ideal case in which simple quantum mechanical calculations can be performed in the SA with analytic wave functions. Recent progress in the production and manipulation of exotic nuclei associated with new trapping techniques allow refined investigations of the β decay of stored ions [12–14]. We present here the first measurement of the SO probability following the β decay of hydrogen-like $^6He^+$ ions. This is a unique system for a comparison with theoretical predictions, which has motivated a careful look at possible systematic effects that could impact the detection of recoiling ions.

The experimental setup has been described in detail elsewhere [13, 15, 16]. Only the main features of the apparatus are presented here along with the modifications which were necessary for the purpose of this measurement. The experiment has been carried out at GANIL, Caen, France. The radioactive ^{6}He nuclei were produced at the SPIRAL target-ECR ion source system. After

mass separation the $^6He^+$ ions were guided at 10 keV through the LIRAT low energy beam line up to the entrance of the LPCTrap apparatus. At this point, the typical $^6He^+$ beam intensity was 10^8 s^{-1}. The first stage of the apparatus is a Radio Frequency Cooler and Buncher (RFQCB) [17] for the beam preparation. This linear Paul trap is mounted on a high voltage platform whose voltage was set to decelerate the ions down to 50 eV. The system was filled with H_2 buffer gas, at a pressure of 7×10^{-3} mbar, to cool down the ions below 1 eV. The $^6He^+$ ions from LIRAT were continuously injected in the RFQCB and accumulated into bunches close to the exit. The cooled bunches were then extracted at a repetition rate of 5 Hz and reaccelerated towards the measurement transparent Paul trap using a pulsed cavity located 12 cm downstream from the exit of the RFQCB. The ions were transported between the two traps with a kinetic energy of about 1 keV and were decelerated down to 100 eV by a second pulsed cavity located at the entrance of the measurement Paul trap. The ions were confined in this trap

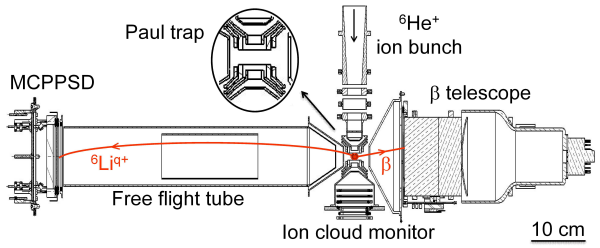

FIG. 1: Top view of the experimental setup. The insert shows the structure of the six stainless steel rings of the Paul trap. See text for details.

(Fig. 1) by a 1.15 MHz RF voltage of 120 V_{pp} applied continuously to the two inner rings. The intermediate rings were set to ground potential and the outer rings were set at a voltage of 12 V to minimize trapping losses. During the experiment, up to 2×10^4 $^6He^+$ ions were successfully trapped in the measurement trap at each injection cycle, which corresponds to an overall transport and trapping efficiency of 10^{-3}. H_2 buffer gas, at a pressure of 4×10^{-6} mbar, was also used in the trapping chamber to further cool down the trapped ions. The β particles and the recoiling ions resulting from the β decay of the trapped $^6He^+$ ions were detected in coincidence using detectors located around the trap (Fig.1). The β telescope, composed of a 300 μm thick double sided silicon strip detector (DSSSD) followed by a plastic scintillator, provides the position and the energy of the incoming β particles. The signal from the plastic scintillator triggers the acquisition system and defines the reference time for a decay event. Recently, a new recoil ion spectrometer has been built to separate the charge states of the recoiling ions. Ions emitted towards the recoil spectrometer cross a first collimator through a 90% transmission grid set at ground potential. They are then accelerated by a -2 kV potential applied to a second 90% transmission grid mounted at the entrance of the free flight tube (Fig.1). Inside this tube, an electrostatic lens at -250 V allows a 100% collection efficiency of the ions, which are detected with a micro-channel plate position sensitive detector (MCPPSD). A -4 kV voltage applied on the front plate of the MCPPSD ensures a maximum detection efficiency for both charge states, independently of the recoil ion initial kinetic energy [19].

For each detected event, the energy and position of the β particle, the time of flight (TOF) and position of the recoil ion, the time of the event within the trapping cycle, and the phase of the trap RF voltage were recorded. In about 25 ms after injection, the trapped ion cloud has reached thermal equilibrium with a final thermal energy $kT \sim 0.1$ eV [18]. After a trapping interval of 150 ms (Fig.2), the ions were extracted towards a second MCPPSD, located downstream from the trap (Fig.1) that serves as a monitor of the ion cloud [15]. The following 50 ms period within the cycle (Fig.2), with no ions in the trap, enables to measure the background for each cycle.

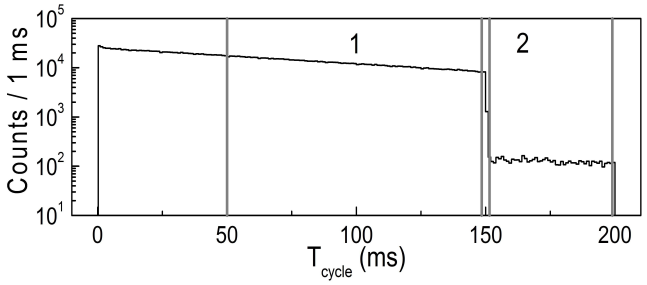

FIG. 2: Coincidence events as a function of time within the trapping cycle. The regions 1 and 2 correspond respectively to the selection of "in-trap" and "out-trap" events.

The procedure applied for the detector calibrations was identical to that described in Ref. [16]. Several conditions were then applied to the data: (1) the energy deposited in the plastic scintillator had to be larger than 0.4 MeV; (2) the signals in the DSSSD must have had a valid conversion corresponding to a minimum ionizing particle; and (3) the signals from the delay lines of the MCPPSD should provide an unambiguous determination of the ion impact position. Two different sets of events were selected using the detection time, $T_{\rm cycle}$, of events within the trapping cycle (Fig.2). The $50 \leq t_{\rm cycle} \leq 149$ ms interval contains decay events from trapped ions having reached thermal equilibrium whereas, in the interval $151 \leq t_{\rm cycle} \leq 200$ ms, the Paul trap was emptied so that only background events were recorded. Such events, called "out-trap" events, result from the decay of neutral ^6He atoms in the detection chamber. This background contribution was less than 1% of the recorded data. After normalization, the background events were subtracted

from those in the first time interval, which contains the events of interest. The resulting TOF spectrum is shown in Fig.3. The regions labeled 1 and 4 contain only acci-

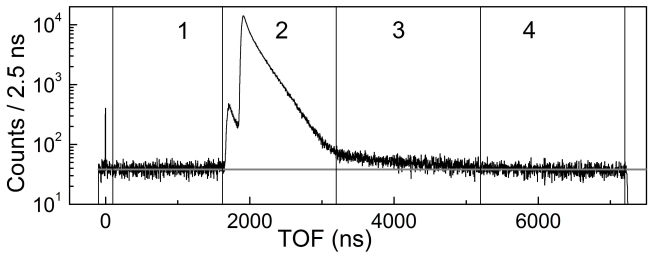

FIG. 3: TOF spectrum of recoil ions. The four regions used in the data analysis are delimited by vertical lines. The horizontal gray line indicates the average level of accidental events.

dental events associated with uncorrelated signals from the β detector and from the MCPPSD. These events are used for the accidentals subtraction from region 2, where the distributions corresponding to $^6Li^{3+}$ and $^6Li^{2+}$ recoil ions are clearly visible. The tail observed in region 3 arises from recoil ions neutralized and scattered by metallic surfaces prior to entering the acceleration region of the spectrometer. These events have a minimum TOF of 3.2 μs and are excluded from the selected data.

The data analysis is similar to the one detailed in Ref. [16], and is based on the comparison between the experimental TOF spectrum and two sets of Monte-Carlo (MC) simulated spectra obtained for $^6Li^{2+}$ and for $^6Li^{3+}$ recoil ions. For both sets, the β decay kinematics was accurately incorporated, using the $\beta\nu$ angular correlation coefficient predicted by the Standard Model, including radiative corrections terms [20]. The initial positions and velocities of the decaying ions were sampled accordingly to distributions obtained from simulations of the motion of trapped ions in the Paul trap, in the presence of H_2 buffer gas. The $^6Li^{2+}$ and $^6Li^{3+}$ paths from the decay point to the MCPPSD were computed using the SIMION8 software. The paths of the β particles were computed with the GEANT4 toolkit to account for the scattering on the electrodes of the Paul trap and on the detectors. The response functions of the β telescope and of the MCPPSD were also included in the MC simulation. It has previously been shown [21] that the shape of the TOF spectrum strongly depends on the ion cloud temperature and on the ions flight distances. The whole simulation was therefore carried out assuming different cloud temperatures around $kT = 0.1$ eV, and for different positions of the MCPPSD relative to the trap. After subtraction of background and accidental events, the experimental TOF spectrum was fitted with a linear combination of the simulated spectra corresponding to the two charge states (Fig.4). The free parameters of the fit are: a global normalization, the electron SO probability, P_{so}^{exp}, the ion cloud temperature, and the distance of the MCPPSD from the trap center. The best fit (Fig.4) has a chi-square at the minimum of $\chi^2 = 533$ for 523 degrees of freedom, which corresponds to a P-value of 0.37. This indicates a very good statistical consistency between the data and the model. The fit leads to an electron SO prob-

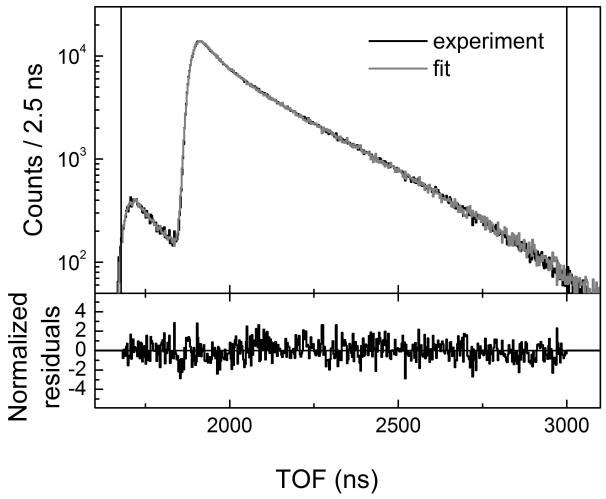

FIG. 4: Upper panel: Fit of the experimental spectrum with the MC simulations. The range selected for the fit is indicated by the vertical lines. Lower panel: Normalized residuals of the fit.

ability $P_{so}^{exp} = 0.02339 \pm 0.00035$, where the quoted error is purely statistical at one standard deviation. Comparisons between the simulations and the experimental data have been performed using other observables, like the position profiles in both detectors and the β energy spectra, and also show a good agreement. The main sources of systematic effects, including the calibration and position accuracy of the detectors, the high-voltage power supply accuracy, background subtraction, and charge exchange on H_2 buffer gas, have been investigated. The detection efficiency of the MCPPSD for the two charge states was determined from the gaussian shapes of the associated measured charges [19]. The efficiency for $^3Li^{3+}$ was found to be $(0.38 \pm 0.05)\%$ larger than for $^3Li^{2+}$ and has been included. Effects giving a contribution larger than 10^{-5} to the uncertainty on P_{so}^{exp} are listed in Table I. The methodology used to estimate these effects is detailed in Ref. [16]. The total systematic uncertainty, 7.0×10^{-5}, is very small compared to the statistical error.

The electron SO probability in an hydrogen-like system is a standard application of the SA and can be calculated following e.g. Ref. [22]

$$P_{so} = 1 - \sum_{n,l,m} \mid \langle 1,0,0,Z \mid \exp(-i\vec{K}\vec{r}) \mid n,l,m,Z' \rangle \mid^2, \quad (1)$$

where n, l and m are the radial, orbital momentum and orbital momentum projection numbers respectively, $Z = 2$ ($Z' = 3$) is the number of protons in the initial (final) system and $\vec{K}$ is the wave vector of the final

TABLE I: Dominant sources of systematic effects along with the size of the correction of $P_{\rm so}^{\rm exp}$ if any (second column), the impact on the error on $P_{\rm so}^{\rm exp}$ (third column) and the method used to estimate the parameters (fourth column).

Source	Corr. (10^{-5})	Error (10^{-5})	Method
$a_{\beta\nu}$	-	4.0	[20]
β scattering	39	4.0	GEANT4
Background	-	3.5	present data
E_β calibration	-	1.7	present data
MCP efficiency	-9	1.2	present data
Total	30^a	7.0	

[a]The size of the corrections are given for indication. The instrumental effects were actually incorporated in the MC fit, so that the value of $P_{\rm so}^{\rm exp}$ obtained from the fit includes these corrections.

system. For the SO following the β decay of ^{6}He$^+$ ions, this leads to

$$P_{\rm so} = (2.33810 + 0.00412 E_{\rm rec}) \times 10^{-2}, \qquad (2)$$

where $E_{\rm rec}$ is the recoil energy of the daughter nucleus expressed in keV. The calculations were performed applying 10^4 non-relativistic hydrogen-like wave functions with different values of n, l and m. The reached numerical accuracy was smaller than 10^{-8}.

Next, a correction to the SA probability was estimated to account for the finite duration of the potential change, which also includes the direct collision mechanism. It was assumed that the β particle travels at the speed of light and that its wave function is distributed on a thin spherical shell with radius $R = ct$. Therefore, the effective perturbation interaction, $\delta V(r, R)$, between the β particle and the orbital electron has a constant value, e^2/R, inside the sphere and the Coulomb form, e^2/r, outside the sphere of radius R. The time dependent Schrödinger equation was solved perturbatively, with an unperturbed Hamiltonian taken for the hydrogen-like ^{6}Li^{2+} ion [22]. The variation in the SO probability was estimated from

$$\delta P_{\rm so} = -\frac{1}{(\hbar c)^2} \int_0^{R_0} dR_1 \int_0^{R_0} dR_2 \, \langle 1s, Z|\delta V(r, R_1)\delta V(r, R_2)|1s, Z\rangle, \qquad (3)$$

where $R_0 = 2\langle 1s, Z|r|1s, Z\rangle$ is the radius of a sphere containing 93% of the electron charge. This leads to the value $\delta P_{\rm so} = -20 \times 10^{-5}$, which is a 1% relative correction to the dominant value obtained in the SA. Such a small correction was indeed expected for a fast process like nuclear beta decay. Substituting in Eq.(2) the mean recoil energy of the events selected in the experimental data analysis (whose error contribution is negligible) together with the correction from Eq.(3) leads to

$$\langle P_{\rm so} \rangle = 0.02322. \qquad (4)$$

The final experimental result obtained in this work,

$$P_{\rm so}^{\rm exp} = 0.02339 \pm 0.00036, \qquad (5)$$

is in perfect agreement with the theoretical result above and with a previous calculation [10]. The measured value is however inconsistent, by 10σ, with the ionization probability per electron of the K-shell estimated by Feinberg for $\epsilon = Z'/Z = 3/2$, $W_K = 0.01983$ [5].

In conclusion, we have reported the first measurement of the SO probability following the β decay of hydrogen-like ions. The decay of ^{6}He$^+$ ions is a unique system that fulfills all conditions to perform a precision comparison between the experimental result and simple, albeit complete, quantum mechanical calculations. Such conditions are: a single active bound electron, a very fast change of the central potential and a resultant pure shake-off process not affected by secondary ionizations like Auger emissions. At the present level of precision, the experimental result was found to be consistent with the theoretical prediction.

We warmly thank Bernard Pons for fruitful discussions that eventually led to the submission of this article. We express our gratitude to G. Darius and M. Herbane for their contributions at an earlier stage of the setup. We are indebted to the LPC staff for their strong involvement in the LPCTrap project and to the GANIL staff for the preparation of a high quality ion beam. K.S.-I. and Z.P. acknowledge the financial support from Narodowe Centrum Nauki (Poland) grant No. 2011/01/B/ST2/05131.

* Electronic address: flechard@lpccaen.in2p3.fr

[1] M. Freedman Ann. Rev. Nucl. Sci. **24**, 209 (1974).
[2] J.A. Tanis *et al.*, Phys. Rev. Lett. **83**, 1131 (1999).
[3] R. Wehlitz *et al.*, Phys. Rev. Lett. **67**, 3764 (1991).
[4] T.Y. Shi and C.D. Lin, Phys. Rev. Lett. **89**, 163202 (2002).
[5] E.L. Feinberg, J. Phys. (USSR) **4**, 423 (1941).
[6] A.B. Migdal, J. Phys. (USSR) **4**, 449 (1941).
[7] J.S. Levinger, Phys. Rev. **90**, 11 (1953).
[8] T.A. Carlson *et al.*, Phys. Rev. **169**, 27 (1968).
[9] N. Scielzo *et al.*, Phys. Rev. A **68**, 022716 (2003).
[10] L. Wauters and N. Vaeck, Phys. Rev. C **53**, 497 (1996).
[11] T.A. Carlson *et al.*, Phys. Rev. **129**, 2220 (1963).
[12] Yu.A. Litvinov *et al.*, Phys. Rev. Lett. **99**, 262501 (2007).
[13] X. Fléchard *et al.*, Phys. Rev. Lett. **101**, 212504 (2008).
[14] V. Kozlov *et al.*, Nucl. Instrum. Methods Phys. Res. B **266**, 4515 (2008).
[15] D. Rodríguez *et al.*, Nucl. Instrum. Methods Phys. Res. A **565**, 876 (2006).
[16] X. Fléchard *et al.*, J. Phys. G: Nucl. Part. Phys. **38**, 055101 (2011).
[17] G. Darius *et al.*, Rev. Sci. Instrum. **75**, 4804 (2004).
[18] X. Fléchard *et al.*, Hyperfine Interact. **199**, 21 (2011).
[19] E. Liénard *et al.*, Nucl. Instrum. Methods Phys. Res. A **551**, 375 (2005).
[20] F. Glück, Nucl. Phys. A **628**, 493 (1998).

[21] P. Velten *et al.*, Hyperfine Interact. **199**, 29 (2011).
[22] L.D. Landau and E.M. Lifshitz, *Quantum Mechanics Non-Relativistic Theory*, Butterworth-Heinemann, Oxford, 1981.